Geochemistry Geophysics Geosystems G3

Research Letter
Volume 11, Number 9
23 September 2010
Q09009, doi:10.1029/2010GC003067
ISSN: 1525-2027

Published by AGU and the Geochemical Society

Indian summer monsoon and winter hydrographic variations over past millennia resolved by clay sedimentation

Onkar S. Chauhan
National Institute of Oceanography, CSIR, 403004 Goa, India (onkar@nio.org)

A. M. Dayal
National Geophysical Research Institute, Uppal Road, 500007 Hyderabad, India

Nathani Basavaiah
Indian Institute of Geomagnetism, 410218 Navi Mumbai, India

U. Syed Abdul Kader
National Institute of Oceanography, CSIR, 403004 Goa, India

[1] Reconstruction of century-scale Indian monsoon and winter hydrography is made from an AMS-dated core located in the unique region of the southeast Arabian Sea which lies in the pathways of the low-salinity Bay of Bengal Waters, advecting during winter northeast monsoon (NEM). Based upon clay mineral analyses in seawaters, we identify chlorite and kaolinite as specific clays supplied by the Bay of Bengal Waters and local fluvial flux (by the southwest monsoon (SWM) precipitation from the Peninsular India), respectively, along the southwest continental margin of India. An evaluation of clay flux and δ^{18}O in *G. ruber* portrays century-scale weaker SWM precipitation events during ~450–650 yr, ~1000 yr, and 1800–2200 cal yr BP. Kaolinite wt % and flux were found to be low during all these events, though chlorite had a persistent or enhanced flux. From the enhanced flux of chlorite and reduced kaolinite/chlorite ratio, during weaker phases of SWM, we deduce a stronger NEM (winter hydrography), implying an inverse coupling between the summer and the winter monsoon.

Components: 5900 words, 7 figures, 2 tables.

Keywords: Bay of Bengal Waters; Indian summer monsoon; winter hydrography; suspended load; clay sedimentation; southeast Arabian Sea.

Index Terms: 0473 Biogeosciences: Paleoclimatology and paleoceanography (3344, 4900); 0429 Biogeosciences: Climate dynamics (1620); 1616 Global Change: Climate variability (1635, 3305, 3309, 4215, 4513).

Received 29 January 2010; **Revised** 19 July 2010; **Accepted** 29 July 2010; **Published** 23 September 2010.

Chauhan, O. S., A. M. Dayal, N. Basavaiah, and U. S. A. Kader (2010), Indian summer monsoon and winter hydrographic variations over past millennia resolved by clay sedimentation, *Geochem. Geophys. Geosyst.*, *11*, Q09009, doi:10.1029/2010GC003067.

1. Introduction

[2] The Indian Monsoon System (IMS), composed of the southwest (SWM) and the northeast monsoons (NEM), is the main source of precipitation on the Indian Subcontinent. Regional variability in precipitation and wind regime associated with IMS shapes a host of marine processes in the northern

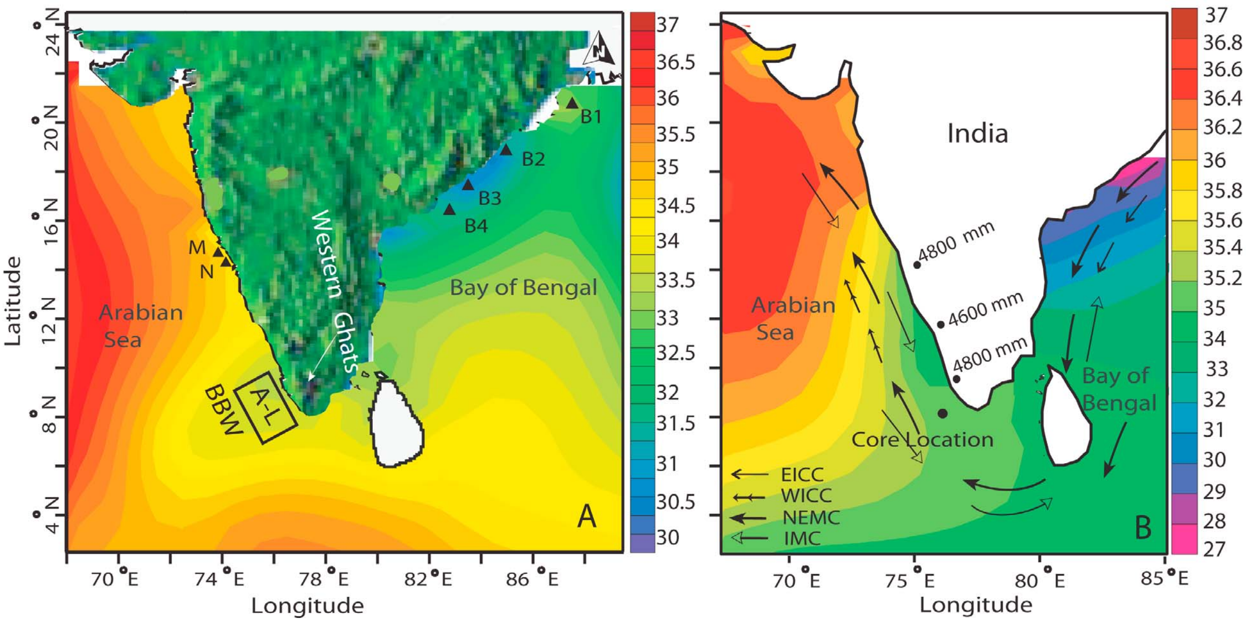

Figure 1. Location of core and seawater samples from the Bay of Bengal (B1–B4) and the Arabian Sea (A–N; refer to Figure 3 for individual locations of water samples A–L marked as a box in Figure 1a). Also shown are regional sea surface salinity (p.s.u) during (a) NEM (December) and (b) SWM (August) together with prevalent hydrography [*Levitus et al.*, 1994]. In Figure 1a, the regional topographic feature the Western Ghats (data from http://web.ics.purdue.edu/~braile/edumod/sv/1down.htm) is shown along the west coast of India (which induces orographic influence on SWM precipitation). The reported measured precipitation during SWM at selected locations is shown in Figure 1b. In Figure 1b, EICC denotes East India Coastal Current, WICC denotes West India Coastal Current, NEMC denotes North East Monsoon Current, and IMC denotes Indian Monsoon Current.

Indian Ocean. For example, a large hydrological imbalance due to precipitation-evaporation (P-E) and fluvial influx associated with hydrometeorological regimes in two adjacent basins (the Bay of Bengal, P $\gg$ E due to higher fluvial runoff and precipitation; the Arabian Sea, excess evaporation and loss of fresh water; E $\gg$ P) leads to an inter-basin transfer. During boreal summer (June through September), the Indian Monsoon Current advects high-salinity Arabian Sea Waters into the Bay of Bengal [*Vinayachandran et al.*, 1999]. Upon cessation of SWM, during NEM (November through February), westward flowing North Equatorial Current as well as the southward flowing East India Coastal Current carry warm, low-salinity, nutrient-rich Bay of Bengal Waters (BBW) into the Arabian Sea [*Prasanna Kumar et al.*, 2004] (Figure 1). The southwest continental margin of India is anomalous because its sea surface salinity and productivity are influenced and regulated by SWM as well as by NEM, and is highly hypoxic [*Prasanna Kumar et al.*, 2004]. Understanding of the dynamics of IMS is, therefore, critical for the agrarian and maritime economy of southeast Asia. However, few continuous records are available for the Late Holocene for comparison with historical or instrumental records. Derived from δ^{18}O variability from cave stalagmite, studies by *Fleitmann et al.* [2003, 2007] and *Sinha et al.* [2007] are the only annually resolved archives of SWM dynamics during the Middle-Late Holocene.

[3] Along the southwest continental margin of India, associated with the presence of regional topographic high the Western Ghats (Figure 1a), there is excessive precipitation induced by condensation of moisture from the SWM winds when these encounter the land. Intense precipitation (about 4800 mm; Figure 1b) during SWM reduces sea surface salinity over the entire southeast Arabian Sea, which remains low during NEM as well due to intrusion of the Bay of Bengal Waters into this region (values 34–33‰; Figure 1). The δ^{18}O variability in surface dwelling planktonic foraminifers archives a composite influence of these monsoon effects.

[4] We have explored the possibility to estimate magnitude of SWM and NEM (through the strength of the Bay of Bengal Waters) by using a new proxy. The composition of clays is controlled by geology, drainage and climate of hinterland [*Weaver*, 1989], and each of fluvial source and ocean water is

Table 1. Calibrated Radiocarbon (Beta Counting and AMS) Ages for Core 167/1[a]

Midlevel (cm)	Sample Lab ID	Material	Method	^{14}C Age (years BP)	Calibrated Age (years BP)	1 SD (years)
10	RG1673904/1	foraminifers[b]	beta counting[b]	840	460	90
13	POZ-22003	*G. ruber*	AMS	950	590	50
14	POZ-22021	*G. ruber*	AMS	1050	630	40
15	RG1673904/2	foraminifers	beta counting	1160	710	30
20	RG1673904/3	foraminifers	beta counting	1440	960	110
24	RG1673904/4	foraminifers	beta counting	1600	1140	100
28	RG1673904/5	foraminifers	beta counting	1760	1300	30
30	RG1673904/6	foraminifers	beta counting	1870	1370	40
38	RG1673904/7	foraminifers	beta counting	2190	1730	110
42	POZ-22062	*G. ruber*	AMS	2450	2020	50
46	POZ-22064	*G. ruber*	AMS	2730	2350	30
50	RG1673904/8	Foraminifers	beta counting	2940	2600	130

[a]*Stuiver and Braziunas* [1993] and http://calib.qub.ac.uk/calib/.
[b]Unbroken mixed species planktonic foraminifers.

expected to have a specific assemblage [*Konta*, 1985]. Along the southwest continental margin of India, we expect to have distinct clay assemblages in the Bay of Bengal Waters as well as in the local fluvial sources solely fed by SWM. We have measured clays in the seawaters of the Bay of Bengal and in the Arabian Sea (in and out of the of the advection path of the Bay of Bengal Waters) to identify clay fluxes specific to SWM and NEM. We explore application of $\delta^{18}O$ and temporal variations in the flux rate of specific clays of SWM and NEM as potential proxies to reconstruct variability in SWM and NEM in a core located in the advection pathways of the Bay of Bengal Waters (Figure 1b). We have chosen the more stable Upper Holocene (last 3 ka) period in which there is a minimal global ice volume effect, and local sea surface temperature and salinity are influenced mostly by IMS [*Duplessy*, 1982; *Rostek et al.*, 1993; *Saher et al.*, 2007].

2. Methodology

[5] For determining specific temporal variations in the magnitude of SWM and NEM, an appropriate site is a prerequisite. However, except for the even inner shelf (~30 m), the entire uneven middle-outer shelf of the southeast Arabian Sea has coarse and unconsolidated relict carbonate detritus (age >8 ka [*Vora et al.*, 1996]). Furthermore, the most of the western margin of India is known to witness mass wasting and slumping [*Chauhan and Almeida*, 1993], which curtails possibility of obtaining several, suitable, high sedimentation, and turbidity free cores from the location that receives intense orographically enhanced precipitation induced fluvial flux and lies also in the advection path of the Bay of Bengal Waters. During several expeditions of the RV *Gaveshani*, and the ORV *Sagar Kanya*, ~23 cores have been collected along the southwest continental margin of India. Several of these exhibit rather slow rate of sedimentation or with reversal of ages in the upper core surfaces. Core RVG 167/1 (3904; latitude 08° 07.9′ N; longitude 76° 01.8′ E; water depth 1400 m; Figure 1) has been found suitable for the present study, because (1) it lies in an area receiving orographically enhanced SWM precipitation; (2) it is located in advection path of the Bay of Bengal Waters, beyond the shelf break (in an area not influenced by any anomalous clay flux through bed load); (3) the overlying waters are anoxic, and expected to retard bioturbation which could disrupt the fine resolution signature [*Qasim*, 1977]; and (4) it has the highest rate of sedimentation. We have obtained 44 subsamples in upper 58 cm of the core.

[6] To constrain the sediment flux rate, a close interval age control is necessary. The core was dated at 4–6 cm intervals (8 levels) by beta counting radiocarbon dates (Table 1). Carbonate bulk ages suffer mostly from contamination from older carbonates. The western continental margin of India has massive carbonates on the outer shelf [*Vora et al.*, 1996], which may be a potential source of contamination in the study area. In order to minimize influence of any possible contamination from older carbonates, the ages were determined on hand picked, mixed species of unbroken planktonic foraminifers. We have improved our age model with four additional AMS ages obtained on specific events of reduced precipitation (Poznan radio carbon laboratory, Poland) on *G. ruber* (250–415 μm size). The ages are converted to the calendar years after necessary correction of 400y for reservoir effect [*Stuiver and Braziunas*, 1993] using Calib program (http://calib.qub.ac.uk/calib/). Narrower interval measurements (4–6 cm) have helped us to

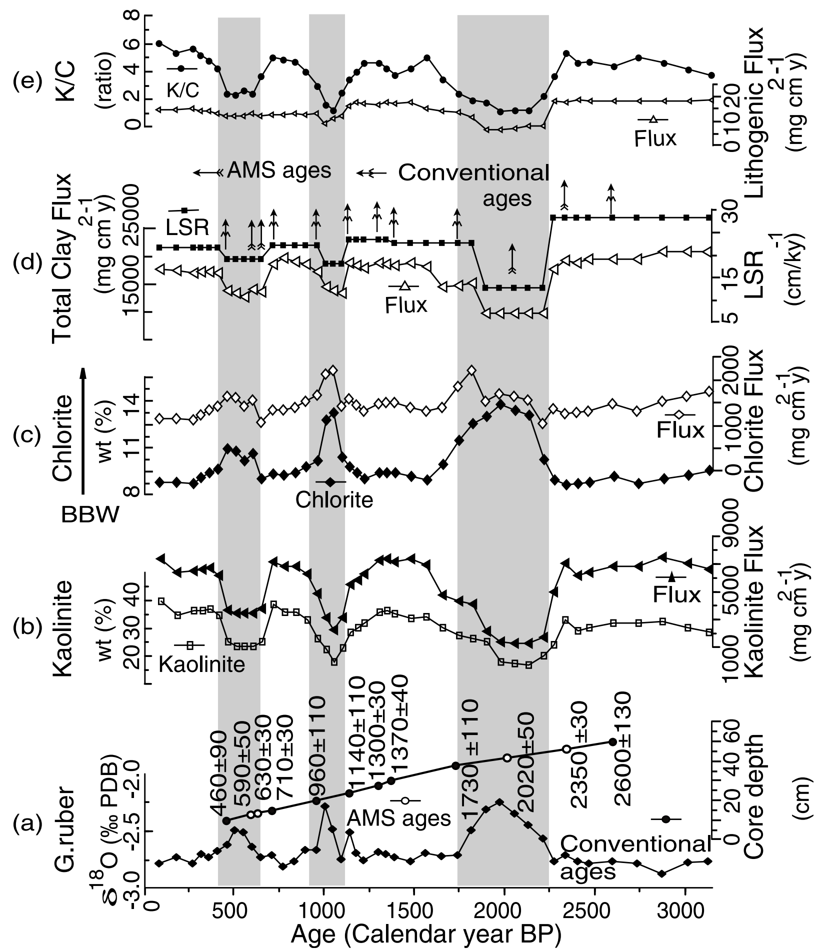

Figure 2. Temporal variations in (a) $\delta^{18}O$ of *G. ruber* together with ^{14}C ages versus depth, (b) kaolinite (flux and wt %), (c) chlorite (flux and wt %), (d) total clay flux rates and linear sedimentation rates (LSR), and (e) K/C ratio and lithogenic flux. Positive relations among heavier $\delta^{18}O$, kaolinite, and K/C ratio during weaker SWM at 450–650, 1000, and 1800–2200 yr BP during enhanced BBW (higher chlorite) are marked with gray shading.

reduce the chronometric error associated with interpolation between longer core intervals (Figure 2). They have also improved estimates of the mass accumulation rate for each specific event. Density variations are important inputs for flux estimation. In order to aid estimation of flux rate, density was measured at 4–6 cm intervals. Sediment samples (known volume) were weighed after drying at 50°C. Dry bulk density is obtained from [*Curry and Lohmann*, 1986]:

$$\text{Dry weight}/\text{Wet volume}$$

The $\delta^{18}O$ of the 25–35 tests of white *G. ruber* (size 315–400 μm, crushed, ultrasonic cleaned in ethanol) was determined at NGRI, Hyderabad and at the University of Kiel. The in-run precision is 0.04‰. Based on repeat measurements (three times daily) of an internal calcite standard (Z-Carrara), external precision on $\delta^{18}O$ measurements is better than ±0.1‰.

[7] In order to identify source specific clays during SWM and NEM (in the load of the Bay of Bengal Waters), suspended load (TSM) and clays at 18 stations were collected from the inner shelf and the upper slope during November 2007 (NEM) and July 2009 (SWM). Four stations are located in the Bay of Bengal; 12 along the study area; 2 in the area farther north with similar SWM precipitation regime but not in the advection path of the Bay of Bengal Waters; see Figure 1 and Table 2. Conventionally, seawater is filtered through a 0.45 μm membrane filter paper to estimate TSM. In addition, we have used a six foot, Prep/Scale TFF regenerated cellulose cartridge (No. CDUF 006 Lm) and a tangential flow filtration system of Millipore to separate particulate matter (size 0.02 μm) from

Table 2. Locations of the Samples, Clays, and TSM in the Seawaters From BOB and the Arabian Sea During NEM and SWM

Station[a]	Location	Depth (m)	Smectite (wt %) NE	Smectite (wt %) SW	Chlorite (wt %) NE	Chlorite (wt %) SW	Illite (wt %) NE	Illite (wt %) SW	Kaolinite (wt %) NE	Kaolinite (wt %) SW	Gibbsite (wt %) NE	Gibbsite (wt %) SW	TSM (mg/l) NE	TSM (mg/l) SW
A	8°04N, 77°30E	12	9	trace	nil	nil	20	12	63	70	trace	12	46	108
B	8°27N, 77°03E	15	8	trace	nil	nil	23	12	63	76	trace	11	48	122
C	8°03N, 76°84E	120	5	22	9	nil	23	19	59	46	trace	11	26	28
D	8°01N, 76°59E	400	22	25	12	nil	26	25	38	38	trace	7	14	24
E	8°44N, 76°56E	80	7	trace	8	nil	28	16	55	68	trace	12	26	35
F	8°24N, 76°36E	1100	19	22	11	nil	42	31	24	37	trace	7	14	18
G	8°43N, 76°22E	800	19	27	21	nil	40	28	18	37	trace	8	16	16
H	8°45N, 76°56E	180	20	23	nil	nil	43	20	32	45	trace	9	28	38
I	8°90N, 76°46E	30	trace	trace	nil	nil	22	12	69	66	trace	11	52	115
J	9°13N, 76°47E	25	5	trace	nil	nil	24	10	64	72	trace	12	54	102
K	8°96N, 76°21E	150	28	16	12	nil	20	24	38	53	trace	7	20	36
L	8°88N, 75°77E	1200	21	26	14	nil	27	31	36	34	trace	7	14	16
M	14°35N, 74°06E	92	20	13	nil	nil	16	43	61	29	trace	9	58	82
N	14°10N, 74°31E	72	22	5	nil	nil	18	22	55	74	trace	trace	64	74
B1	21°08N, 87°72E	52	13	8	20	29	51	52	8	9	nil	trace	58	87
B2	19°12N, 85°60E	60	19	8	19	23	53	60	7	7	nil	trace	74	103
B3	17°54N, 83°33E	82	9	7	22	21	65	64	trace	6	nil	trace	65	92
B4	16°51N, 82°34E	74	8	9	21	22	57	58	12	9	nil	trace	68	102

[a]A–N, Arabian Sea; B1–B4, Bay of Bengal (refer to Figures 1 and 3).

seawater. For clay minerals analysis, the separated matter was passed through microplated sieves of 15 μm. The separated <15 μm fraction was first treated with mild acetic acid (10%) and hydrogen per oxide to remove carbonate and organic matter. After several washing to remove the reagents from solution, it was filtered through a 2 μm membrane filter. The clays retained on filter paper were dispersed on a glass slide, and air-dried to obtain an oriented sample. *Carroll* [1970] has suggested treatment with ethylene glycol (glycolation) for expandable clays at 60°C for 1 h. Considering the small quantity of clay fraction, we have glycolated our samples at 100°C for 2 h to resolve duplet of chlorite and smectite. Replicate samples were heated in stages at 300, 600 (575–625), and 650°C in a muffle furnace for 1 h to identify smectite, kaolinite and chlorite [*Carroll*, 1970]. Glycolated and heat treated samples were analyzed on an X-ray diffractometer (model: Phillips 1840) using Ni-filtered Cu Kα radiation (λ = 1.541A°). Clay minerals were identified and quantified using the methods of *Biscaye* [1965] and *Carroll* [1970]. Precision of the analyses is ±8 per cent for smectite and ±5 per cent for other clays.

[8] We have estimated clay flux following *Sirocko and Lange* [1991]:

$$\mathrm{Flux(cl)} = \mathrm{LSR} \times \mathrm{D} \times \mathrm{Wt}$$

where Flux (cl) = flux of the individual clay (mg cm^2 ky^{-1}), LSR = linear sedimentation rate (cm ky^{-1}), D = dry density, Wt = weight percent of an individual clay mineral.

3. Results and Discussions

[9] In our core δ^{18}O varies between −2.79 to −2.29‰ (Figure 2), and excursions toward the heavier δ^{18}O values are observed at 450–650 (~0.24‰), ~1000 (0.45‰), 1800–2200 (0.51‰) cal yr BP (Figure 2). Based upon the criterion of *Sarkar et al.* [2000], these signify sea surface salinity or sea surface temperature variability of >1‰ or >1°C. During past 3 ka, the sea surface temperature variations in the Arabian Sea are rather insignificant [*Rostek et al.*, 1993; *Saher et al.*, 2007]. From the modern salinity/O isotope measurements, *Delaygue et al.* [2001] have found strong relations between salinity and δ^{18}O in the Arabian Sea. We link these incursions, therefore, with sea surface salinity enhancements. Even though *G. ruber* is surface dwelling and proliferates throughout the year [*Saher et al.*, 2007], SWM had been considered to be the regulator of its δ^{18}O [*Sarkar et al.*, 2000; *Tiwari et al.*, 2006, and references therein]. Owing to advection of low-salinity Bay of Bengal Waters, the δ^{18}O variability in our core will be a composite of SWM as well as NEM component of sea surface salinity changes. There exist no clues to separate out specific influence of BBW on δ^{18}O variability. However, during a weaker SWM phase, associated with reduced fluvial discharge, sea surface salinity

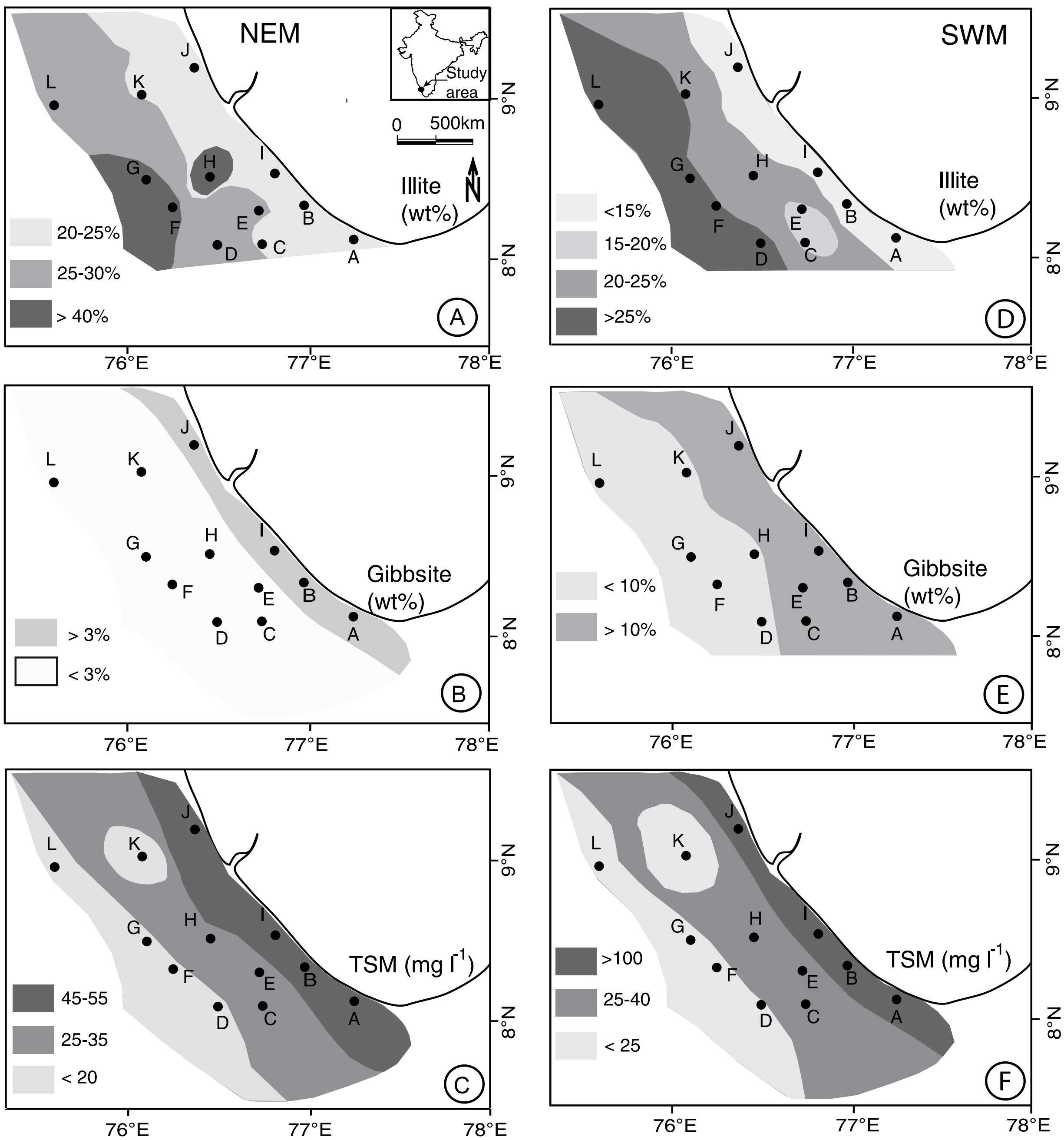

Figure 3. Sampling locations (labeled as A–L) and spatial distributions of TSM and clays measured in surficial seawaters during (a–c) SWM and (d–f) NEM. Figures 3a and 3d are for illite, Figures 3b and 3e are for gibbsite, and Figures 3c and 3f are for TSM. Note the conspicuous absence of chlorite in the entire study area during SWM.

of the Bay of Bengal, and that of BBW is expected to be enhanced. We hypothesize, therefore, that associated with an increase in the salinity of BBW, there will be an overall sea surface salinity enhancement in the Arabian Sea during a weaker phase of SWM. The excursions to heavier δ^{18}O, therefore, are interpreted to result from sea surface salinity enhancement associated with a weaker SWM at 2200–1800, ~1000 and 650–450 yr BP. Our interpretation of the O isotope record is supported by archived data which show precipitation minima and reduced runoff at 2200–1900, 1000 and 650–450 yr BP in the fluvial runoff records of the River Indus [*von Rad et al.*, 1999]. A weaker SWM at 2200–2300 yr has also been reported for the Bay of Bengal [*Chauhan and Suneethi*, 2001]. *Tiwari et al.* [2006] have found a weaker SWM at 550, 1100 and 2000 yr BP from δ^{18}O variability in *G. ruber*. The event of

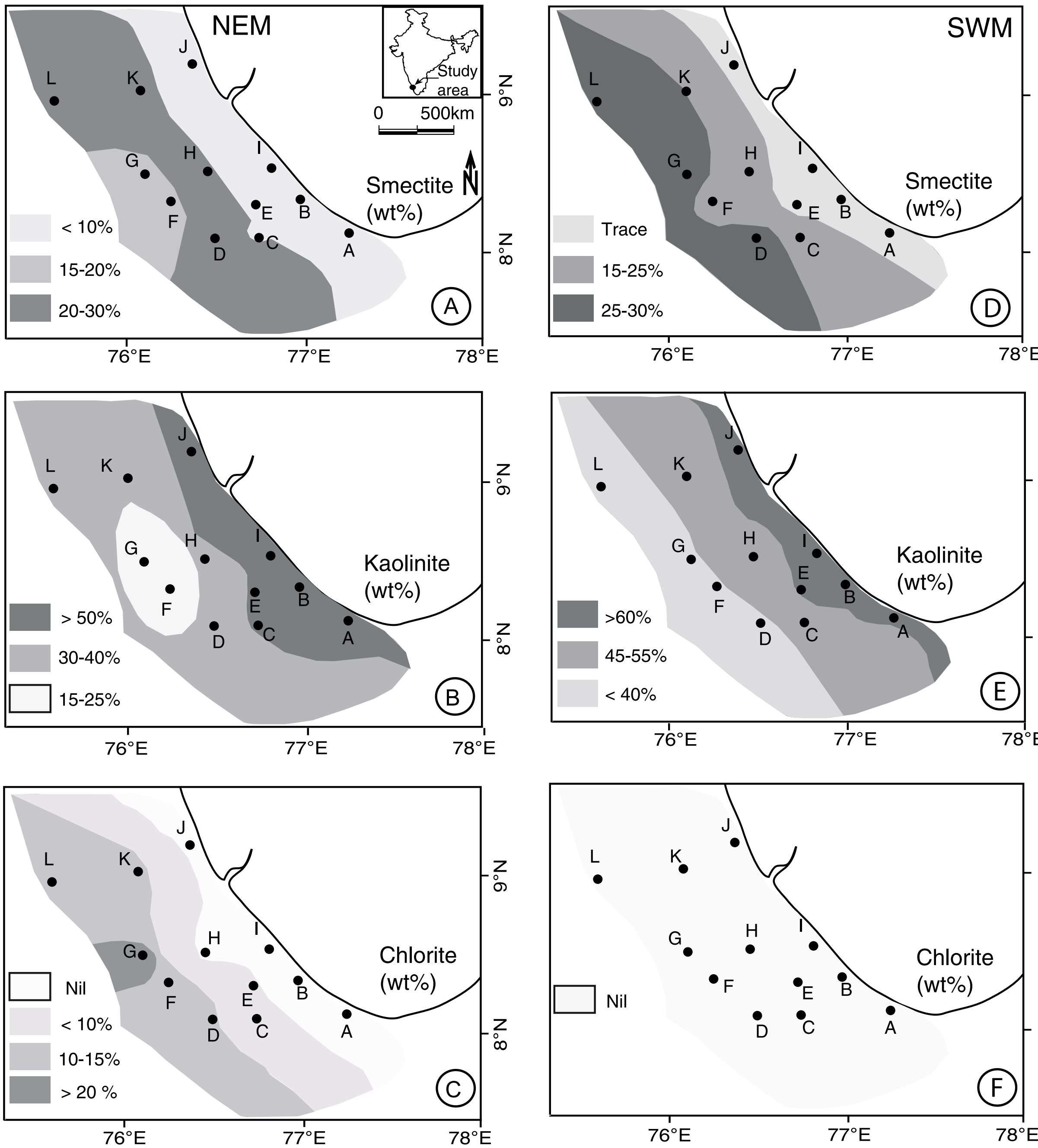

Figure 4. Same as Figure 3 but for (a and d) smectite, (b and e) kaolinite, and (c and f) chlorite.

550 yr BP is archived also in the annually resolved records of stalagmite from the core monsoon region of India [*Sinha et al.*, 2007]. Based on varve thickness, *von Rad et al.* [1999] concluded that fluvial flux of the Indus was enhanced during 1200–1700 and 2600 yr BP. A stronger SWM during <400 y and 600–1200 yr BP was inferred from wind induced upwelling proxies of the western Arabian Sea [*Anderson et al.*, 2002; *Gupta et al.*, 2003] which is concurrent with stronger SWM archived in our studies. We therefore infer that incursions to heavier O isotopic composition in our studies are the result of regionally weaker SWM phases.

[10] Our reconstruction based on clay mineral abundance also supports this model. Clays less than ~2 μm in size can be transported over long distances. Their production and supply is dependent

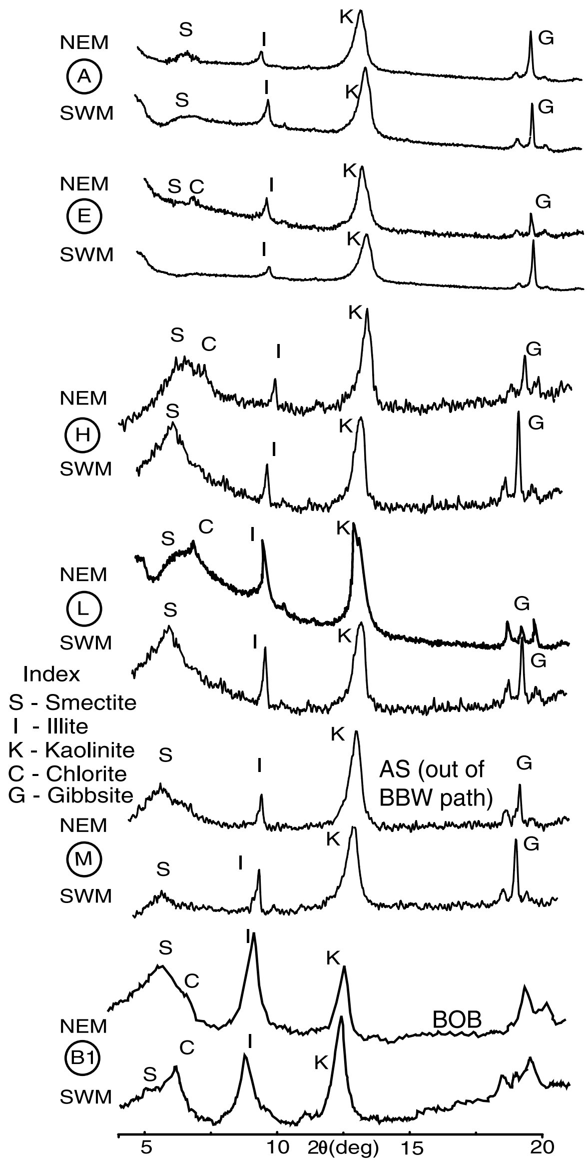

Figure 5. Selected X-ray diffractograms from the Bay of Bengal and the Arabian Sea during SWM and NEM for selected stations (refer to Figures 1a and 3 and Table 2). Note the absence of chlorite at stations A, E, H, L, and M from the Arabian Sea during SWM.

on geology, drainage and climate [*Weaver*, 1989], and therefore they potentially can be used as climate proxy and geotracers [*Biscaye*, 1965; *Weaver*, 1989; *Chauhan and Gujar*, 1996; *Chauhan et al.*, 2000, 2006]. Chlorite is produced under arid, cold climate due to intense physical weathering. In the Indian subcontinent it is mostly found in the rivers with catchments in the glaciated region of the Himalayas [*Konta*, 1985]. Kaolinite and gibbsite are produced under tropical humid climate by intense chemical weathering [*Weaver*, 1989; *Chauhan and Gujar*, 1996]. The climate of the southwest Peninsular India is tropical humid and about 80% of precipitation in the region occurs during SWM. The Western Ghats has two prominent geological formations. The northern region has Deccan Traps (volcanic rocks) while the southern region (in the vicinity of the study area) has Archaean formations (charnokite, khondalite, gneiss etc) [*Chauhan and Gujar*, 1996, and references therein]. Such geology under tropical humid climate with abundant rain sustains an intense chemical weathering regime, and would aid in production of (1) gibbsite, kaolinite and illite from Archaean formations and (2) smectite, kaolinite and gibbsite from volcanic rocks. These clays are found in soil, estuarine and in shelf sediments along the western continental margin of India; in contrast chlorite is conspicuous by its absence [*Chauhan and Gujar*, 1996, and references therein]. Had there been any production of chlorite in the Western Ghats, it would also be found along with kaolinite and gibbsite in soil, river, estuarine and in seabed samples, which is in fact not the case. It is unlikely therefore that this clay is supplied from the local mountains (the Nilgiris) of the Peninsular India through SWM fluvial flux.

[11] We have evaluated the surficial sediment distribution and physiography of the shelf to get further clues on the source and dispersal pathways of clays. *Chauhan and Gujar* [1996] have found that the middle and the outer shelf are devoid of clays. The shelf has rugged and uneven physiography with exposed relic reef (age >8 ka [*Vora et al.*, 1996]), which implies that the middle-outer shelf is not an active depocenter of modern clays from the load carried over seabed, despite an intense SWM precipitation. We infer therefore that the flux of the clays is through water column processes. In order to affirm this, we have evaluated TSM and clays at 12 stations (Figures 3, 4, and 6 and Table 2) from this area. TSM varies significantly during SWM and NEM in the inland waters (122–46 mg l^{-1}), but it is found low at water depths of more than 40 m (28 to 14 mg l^{-1}; Figures 3, 4, and 6 and Table 2). Low TSM at offshore stations (depth >40 m) affirms further its limited supply to the deeper waters. We attribute this to the prevailing alongshore hydrography (Figure 1), which inhibits across shelf advection of TSM. An entrapment of fines by infragravity edge waves in the coastal waters [*Tatavarti and Narayana*, 2006, and references therein] impedes further supply of fines into the deeper region of the middle-outer shelf. The occurrence of clay-deficient, relict carbonate facies over the middle-outer shelf therefore implies poor

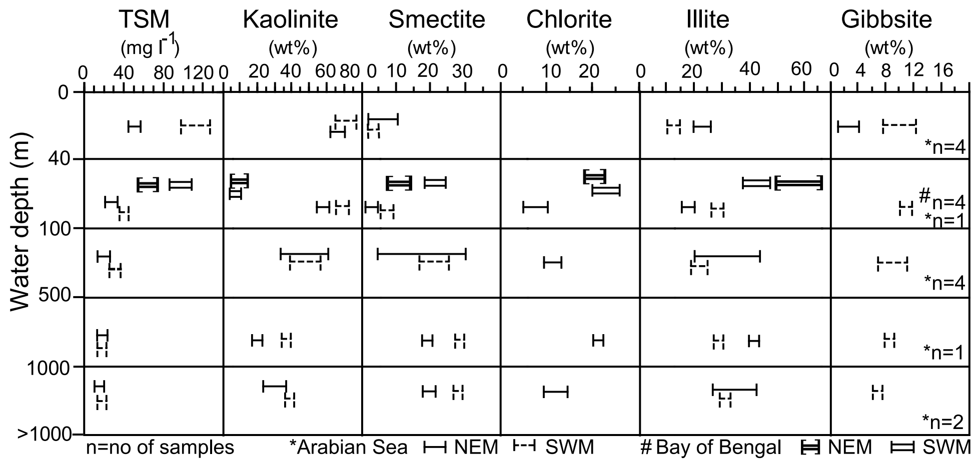

Figure 6. Depth versus TSM and clay abundance during NEM and SWM in the seawaters of the SE Arabian Sea and the Bay of Bengal. Refer to Figure 1 for the locations of the samples. Note offshoreward diminution in kaolinite, though chlorite occurs in the deeper waters (>100 m) during NEM only in the SE Arabian Sea.

sequestering of SWM or NEM fluxes over the shelf due to prevalent hydrographic regime.

[12] The clay assemblage and representative X-ray diffractograms of the seawater TSM during NEM and SWM from the Arabian Sea and the Bay of Bengal are presented in Figures 3–5. The surficial distribution of clays during SWM and NEM are markedly different. During SWM, kaolinite is the predominant clay with illite and gibbsite as minor clays on the entire inner shelf. In contrast, the outer shelf-slope waters were found with kaolinite, illite, and smectite as the most abundant clays with minor gibbsite (Figures 3 and 4), which is very close to the clay assemblages reported in the homogenized surficial sediments in this region [*Chauhan and Gujar*, 1996]. We have found similar assemblage at two other stations (M, N) located farther northward (not in the advection pathways of the Bay of Bengal Waters; Figure 1 and Table 2). At all these stations chlorite is conspicuously absent, which implies that it is not supplied along with kaolinite and gibbsite. In order to substantiate this inference, we have obtained and evaluated water depth versus clays distribution in seawaters during NEM and SWM (Figure 6). We found (1) offshoreward depletion in kaolinite and gibbsite and (2) occurrence of chlorite over the deeper regions during NEM only (Figure 6). Had there been any production of chlorite in the local hills of the Western Ghats, it should have been found also in the shallow seawaters of the shelf during SWM when fluvial discharge (TSM) is at its peak (Figure 6). The conspicuous absence of chlorite in the shallow waters is, therefore attributed to its nonproduction and supply from the Western Ghats.

[13] We have documented occurrence of illite and chlorite in the seawater samples of the Bay of Bengal during NEM as well SWM (Figures 5 and 6). During NEM, we found occurrence of chlorite in seawaters of all the offshore stations from the locations that are influenced by the Bay of Bengal Waters (Figure 1 and Table 2). Because chlorite is absent over the entire shelf during SWM, we attribute its presence during NEM to the Bay of Bengal Waters. In order to validate this inference, we have evaluated correlation among clays in seawater. We found negative correlation between kaolinite versus chlorite ($r = -0.75$; $p = 0.01$), though between kaolinite versus gibbsite it is positive ($r = 0.73$; $p = 0.01$; Figure 7). A negative correlation ($r = -0.76$; $p = 0.001$; $n = 44$) is found also between chlorite and kaolinite in the sediments of the core (Figure 7). A negative correlation between clays known to be produced under arid, cold climate (chlorite) and humid, tropical climate (kaolinite) versus a positive correlation between the kaolinite and gibbsite lead us to infer that chlorite is not produced in the Western Ghats and is supplied via BBW into the SE Arabian Sea during NEM. We, therefore, infer that chlorite is supplied into the core site through the Bay of Bengal Waters. Similarly, kaolinite is contributed through local fluvial sources from the adjacent hills of the Peninsular India, and its supply is equated with the SWM precipitation. The temporal variability in kaolinite and chlorite, therefore, may be linked with intensity of SWM and NEM, respectively. Because a higher (lower) abundance/flux of kaolinite (chlorite) is related with SWM (NEM), we have used kaolinite/chlorite (K/C) ratio also as an index of the magnitude of SWM/NEM.

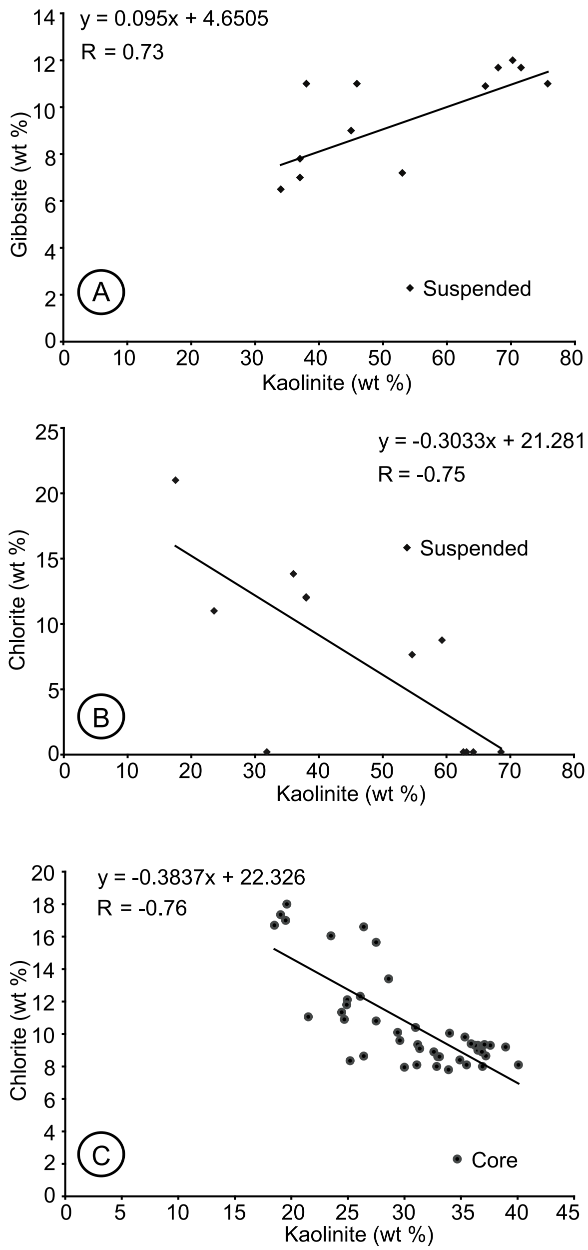

Figure 7. X-Y plots of clays. (a) Correlation between kaolinite and gibbsite and (b) chlorite versus kaolinite in seawaters of the southeast Arabian Sea. (c) Correlation between chlorite and kaolinite in the sediments of the core. Note a negative correlation between chlorite versus kaolinite in seawaters as well as in the sediments of the core.

[14] The total flux of clays is found to be highly variable. In general, the flux is about 17.2–18.9 g cm^2 ky^{-1}. However, during 450–650, 1000 and 1800–2200 cal yr BP, contrary to an overall reduction in kaolinite and in total flux of clays (~13.5 −10.3 g cm^2 ky^{-1}), an enhanced flux of chlorite is observed (Figure 2). Concordant with lighter δ^{18}O (lower sea surface salinity and enhanced SWM) the kaolinite flux was enhanced during >2200, 1800–1100, 900–650 and <400 cal yr BP, and was reduced during all the heavier incursion episodes (reduced SWM precipitation) of 2200–1800, ~1000 and 650–450 cal yr BP. The kaolinite flux is therefore coeval with SWM variability. During a reduced precipitation regime, the fluvial discharge is expected to be diminished with considerable decrease of (1) production and supply of fine detritus, (2) carrying capacity, and (3) overall sedimentation. The enhanced flux of chlorite, when, overall clays and kaolinite fluxes are reduced and sea surface salinity is increased (Figure 2), is anomalous to this dictum. We propose that an increased chlorite flux during weaker phases of SWM (reduced kaolinite flux and heavier δ^{18}O) appears to stem from the prevalence of stronger NE winds due to colder temperature over the Himalayas sustaining a vigorous winter hydrography. In order to validate this hypothesis, we have obtained lithogenic flux rate (from the residue that remained after treatment of bulk sediments with 10% acetic acid) and compared it with that of δ^{18}O, fluxes of chlorite and kaolinite, and K/C ratio (Figure 2). We find reduced lithogenic and clay fluxes during all the events of aridity (Figure 2). Conspicuously, there is an augmentation (reduction) of chlorite (kaolinite and K/C ratio; Figure 2) during these times. From lower lithogenic, kaolinite, total clay flux and heavier δ^{18}O during these events, we deduce a prolonged and substantial reduction in the SWM precipitation curtailing fluvial discharge and the yield of terrigenous detritus. Had chlorite been produced or supplied from the Western Ghats and had a link with SWM, it should have also been reduced also during the events of weaker SWM. An enhanced or persistent flux of chlorite (clay contributed exclusively during NEM only) therefore archives its higher production under arid, cold climate and its augmented supply through intensification of winter hydrography strengthening BBW flux during all these weaker phases of SWM. The observed antiphase behavior between kaolinite and chlorite endorses an inverse coupling between the SWM precipitation and the northward flow of the Bay of Bengal Waters that occurs during the northeast winter monsoon. Because of high nutrients carried in BBW, an augmentation in the marine productivity during advection of BBW has been documented [*Prasanna Kumar et al.*, 2004]. We speculate that an enhanced BBW during weaker SWM phases appears to have implications for

enhanced productivity along the southeast Arabian Sea, which needs to be accounted while estimating past carbon budgets during century-scale events of climate variability.

Acknowledgments

[15] The authors are thankful to the director of the National Institute of Oceanography, Dona Paula, Goa, for providing the facilities. We acknowledge Louis Derry, Vincent Salters, Julian Sachs, and anonymous referees for constructive reviews which have improved the science in the manuscript. We thank the Space Application Center and IGBP-ISRO, Ahmedabad, for financial grants for TSM and clay mineral studies. We acknowledge the support of the Indian Coast Guard. Kumud K. Singh, E. Vogelsang, and M. Saranthein helped with carbon and oxygen analysis and interpretation. This paper is NIO contribution 4677.

References

Anderson, D. M., J. T. Overpeck, and A. K. Gupta (2002), Increase in the Asian southwest monsoon during the past four centuries, *Science*, *297*, 596–599, doi:10.1126/science.1072881.

Biscaye, P. E. (1965), Mineralogy and sedimentation of recent deep-sea clays in the Atlantic Ocean and adjacent seas and oceans, *Geol. Soc. Am. Bull.*, *76*(7), 803–832, doi:10.1130/0016-7606(1965)76[803:MASORD]2.0.CO;2.

Carroll, D. (1970), Clay minerals: A guide to their X-ray identification, *Spec. Pap. Geol. Soc. Am.*, *126*, 80 pp.

Chauhan, O. S., and F. Almeida (1993), Influences of Holocene sea level, regional tectonics, and fluvial, gravity and slope currents induced sedimentation on the regional geomorphology of the continental slope off northwestern India, *Mar. Geol.*, *112*, 313–328, doi:10.1016/0025-3227(93)90176-V.

Chauhan, O. S., and A. R. Gujar (1996), Surficial clay mineral distribution on the southwestern continental margin of India: Evidence of input from the Bay of Bengal, *Cont. Shelf Res.*, *16*, 321–333, doi:10.1016/0278-4343(95)00015-S.

Chauhan, O. S., and J. Suneethi (2001), 18 Ka BP records of climatic changes, Bay of Bengal: Isotopic and sedimentological evidences, *Curr. Sci.*, *81*(9), 1231–1234.

Chauhan, O. S., B. S. Sukhija, A. R. Gujar, N. Nagabhushanam, and A. L. Paropkari (2000), Late quaternary variations in clay minerals along the SW continental margin of India: Evidence of climatic variations, *Geo Mar. Lett.*, *20*(2), 118–122, doi:10.1007/s003670000043.

Chauhan, O. S., S. Jayakumar, A. A. A. Menezes, A. S. Rajawat, and S. R. Nayak (2006), Anomalous inland influx of the River Indus, Gulf of Kachchh, India, *Mar. Geol.*, *229*(1–2), 91–100, doi:10.1016/j.margeo.2005.12.003.

Curry, W. B., and W. G. P. Lohmann (1986), Late quaternary carbonate sedimentation at the Sierra Leone Rise (eastern equatorial Atlantic Ocean), *Mar. Geol.*, *70*, 223–250, doi:10.1016/0025-3227(86)90004-6.

Delaygue, D., E. Bard, C. Rollion, J. Jouzel, M. Stievenard, J. Duplessy, and G. Ganssen (2001), Oxygen isotope/salinity relationship in the northern Indian Ocean, *J. Geophys. Res.*, *106*, 4565–4574, doi:10.1029/1999JC000061.

Duplessy, J. C. (1982), Glacial to interglacial contrasts in the northern Indian Ocean, *Nature*, *295*, 494–498, doi:10.1038/295494a0.

Fleitmann, D., S. J. Burns, M. Mudelsee, U. Neff, J. Kramers, A. Mangini, and A. Matter (2003), Holocene forcing of the Indian monsoon recorded in a stalagmite from southern Oman, *Science*, *300*, 1737–1739, doi:10.1126/science.1083130.

Fleitmann, D., et al. (2007), Holocene ITCZ and Indian monsoon dynamics recorded in stalagmites from Oman and Yemen (Socotra), *Quat. Sci. Rev.*, *26*, 170–188, doi:10.1016/j.quascirev.2006.04.012.

Gupta, A. K., D. M. Anderson, and J. T. Overpeck (2003), Abrupt changes in the Asian southwest monsoon during the Holocene and their links to the North Atlantic Ocean, *Nature*, *421*, 354–357, doi:10.1038/nature01340.

Konta, J. (1985), Mineralogy and chemical maturity of suspended matter in major rivers samples under SCOPE/UNEP project, in *Transport of Carbon and Minerals in Major World Rivers*, part III, edited by E. T. Degens et al., *Mitt. Geol. Palaeont. Inst. Univ. Hamburg*, 58, pp. 569–592, Sci. Comm. on Problems of the Environ., Paris.

Levitus, S., R. Burgett, and T. P. Boyer (1994), *World Ocean Atlas 1994*, vol. 3, *Salinity, NOAA Atlas NESDIS*, vol. 3, 111 pp., NOAA, Silver Spring, Md.

Prasanna Kumar, S., et al. (2004), Intrusion of the Bay of Bengal water into the Arabian Sea during winter monsoon and associated chemical and biological response, *Geophys. Res. Lett.*, *31*, L15304, doi:10.1029/2004GL020247.

Qasim, S. Z. (1977), Biological productivity of the Indian Ocean, *Indian J. Mar. Sci.*, *6*, 122–137.

Rostek, F., G. Ruhlandt, F. Bassinot, P. J. Muller, L. D. Labeyrie, Y. Lancelot, and E. Bard (1993), Reconstructing sea surface temperature and salinity using δ^{18}O alkenone records, *Nature*, *364*, 319–321, doi:10.1038/364319a0.

Saher, M. H., S. J. A. Jung, H. Elderfield, M. J. Greaves, and D. Kroon (2007), Sea surface temperatures of the western Arabian Sea during the last deglaciation, *Paleoceanography*, *22*, PA2208, doi:10.1029/2006PA001292.

Sarkar, A., R. Ramesh, B. L. K. Somayajulu, R. Agnihotri, A. J. T. Jull, and G. S. Burr (2000), High resolution Holocene monsoon record from the eastern Arabian Sea, *Earth Planet. Sci. Lett.*, *177*, 209–218, doi:10.1016/S0012-821X(00)00053-4.

Sinha, A., K. G. Cannariato, L. D. Stott, H. Cheng, R. L. Edwards, M. G. Yadava, R. Ramesh, and I. B. Singh (2007), A 900-year (600 to 1500 A.D.) record of the Indian summer monsoon precipitation from the core monsoon zone of India, *Geophys. Res. Lett.*, *34*, L16707, doi:10.1029/2007GL030431.

Sirocko, F., and H. Lange (1991), Clay-mineral accumulation rates in the Arabian Sea during the late Quaternary, *Mar. Geol.*, *97*, 105–119, doi:10.1016/0025-3227(91)90021-U.

Stuiver, M., and T. F. Braziunas (1993), Modeling atmospheric ^{14}C influences and ^{14}C ages of marine samples to 10000 BC, *Radiocarbon*, *35*(1), 137–191.

Tatavarti, R., and A. C. Narayana (2006), Hydrodynamics in a mud Bank regime during nonmonsoon and monsoon seasons, *J. Coastal Res.*, *22*(6), 1463–1473, doi:10.2112/05-0461.1.

Tiwari, M., R. Ramesh, M. G. Yadava, B. L. K. Somayajulu, A. J. T. Jull, and G. S. Burr (2006), Is there a persistent control of monsoon winds by precipitation during the late Holocene?, *Geochem. Geophys. Geosyst.*, *7*, Q03001, doi:10.1029/2005GC001095.

Vinayachandran, P. N., Y. Masumoto, T. Mikawa, and T. Yamagata (1999), Intrusion of the southwest monsoon current into the Bay of Bengal, *J. Geophys. Res.*, *104*(C5), 11,077–11,085, doi:10.1029/1999JC900035.

von Rad, U., M. Schaaf, K. Michels, H. Schulz, W. Berger, and F. Sirocko (1999), A 5000–year record of climate change in varved sediments from the Oxygen Minimum zone off Pakistan, northeastern Arabian Sea, *Quat. Res.*, *51*, 39–53, doi:10.1006/qres.1998.2016.

Vora, K. H., B. G. Wagle, M. Veerayya, F. Almeida, and S. M. Karisiddaiah (1996), 1300 km long late Pleistocene-Holocene shelf edge barrier reef system along the western continental shelf of India: Occurrence and significance, *Mar. Geol.*, *134*, 145–162, doi:10.1016/0025-3227(96)00029-1.

Weaver, C. E. (1989), *Clays, Muds and Shales, Dev. in Sedimentol.*, vol. 44, Elsevier, Amsterdam.